ORIGINAL ARTICLE

NLRC5 modulates bone metabolism and plays a role in periodontitis

Weiping Wang[1] | **Wenyi Liu**[1] | **Jianru Liu**[1] | **Peiying Lv**[1] | **Yixiang Wang**[2] |
Xiangying Ouyang[1]

[1]Department of Periodontology, Peking University School and Hospital of Stomatology & National Clinical Research Center for Oral Diseases & National Engineering Laboratory for Digital and Material Technology of Stomatology & Beijing Key Laboratory of Digital Stomatology, Beijing, China

[2]Central Laboratory, Peking University School and Hospital of Stomatology & National Clinical Research Center for Oral Diseases & National Engineering Laboratory for Digital and Material Technology of Stomatology & Beijing Key Laboratory of Digital Stomatology, Beijing, China

Correspondence
Y. Wang, Central Laboratory, Peking University School of Stomatology, 22 Zhongguancun South Avenue, Haidian District, Beijing 100081, China.
Email: kqwangyx@bjmu.edu.cn

X. Ouyang, Department of Periodontology, Peking University School of Stomatology, 22 Zhongguancun South Avenue, Haidian District, Beijing 100081, China.
Email: kqouyangxy@bjmu.edu.cn

Abstract

Introduction: NOD-like receptor C5 (NLRC5) plays a significant role in the immune system, and is one of the largest members of the pattern recognition receptor family. Previous studies have found that NLRC5 might be involved in the regulation of various diseases, such as fibrotic diseases and cancers; however, its effect on bone metabolism-related diseases has not been reported.

Methods: Skeletons of $Nlrc5^{-/-}$ mice generated by CRISPR/Cas9 and wild-type (WT) mice were compared using X-ray, micro-computed tomography, double labeling, and histological examination. Tartrate-resistant acid phosphatase and pit-absorption assays were performed to evaluate the effect of NLRC5 on osteoclasts differentiation and osteoclastic capacity. The influence of NLRC5 on osteoblasts differentiation and bone formation were studied using alkaline phosphatase and alizarin red staining, respectively. Experimental periodontitis was induced by *Porphyromonas gingivalis* infection and ligature to investigate the role of NLRC5 in inflammatory periodontal bone loss.

Results: Adenovirus-mediated NLRC5 overexpression in human bone marrow mesenchymal stem cells regulated osteogenesis positively. The femoral osteogenesis ability was significantly weakened in $Nlrc5^{-/-}$ mice. Histology showed that the area of the femoral trabeculae in the $Nlrc5^{-/-}$ mice was less than that in the WT mice, and radiology suggested that the $Nlrc5^{-/-}$ mice had fewer trabeculae and a thinner bone cortex than those of the WT mice. *Nlrc5* knockout decreased osteoblast mineralization and increased osteoclastogenesis in vitro. NLRC5 was downregulated in periodontitis and *P. gingivalis* infection. In the experimental periodontitis model, the alveolar bone loss, inflammatory cell infiltration, and inflammatory cytokines secretion (interleukin [IL]-1β, IL-6, and tumor necrosis factor alpha [TNF-α]) in the $Nlrc5^{-/-}$ mice were significantly enhanced compared to WT mice.

Conclusion: We verified a novel role of NLRC5 in bone metabolism by regulating both osteoclasts activity and osteoblasts activity. Our results revealed a protective effect of NLRC5 against periodontal inflammation and alveolar bone destruction. NLRC5 could be a novel treatment target to prevent periodontal bone destruction.

W. Wang and W. Liu contributing equally to this article.

1 | INTRODUCTION

Bone remodeling is a dynamic equilibrium process maintained by the bone-formation activity of osteoblasts and the bone-resorption activity of osteoclasts. The osteoblasts lineage is differentiated from pluripotent mesenchymal precursors through a complex process involving biomarkers and transcription factors such as osterix and runt-related transcription factor 2 (RUNX2).[1,2] By contrast, osteoclasts are differentiated from mononuclear cells and macrophages. Receptor activator of nuclear factor-kappa B ligand (RANKL) is one of essential factors for osteoclast function by binding to RANK.[3] In response to the inducing stimulator, the pre-osteoclasts line up along the bone surface and then fuse with each other to form a single huge cell.[4] Dendrocyte expressed seven transmembrane protein (DC-STAMP), tartrate-resistant acid phosphatase (TRAP), matrix metalloproteinase 9 (MMP9), and cathepsin K are the important markers of osteoclasts.[5]

Periodontitis is initiated by microbiota plaque and leads to severe destruction of periodontal tissue, which is the most common chronic inflammatory oral disease.[6] However, the molecular networks controlling alveolar bone resorption during periodontitis are not fully understood. The appearance of the field of osteoimmunology in the 21st century reflects the tight interconnection between the immune system and the skeleton, and has focused on the study of alveolar bone loss in periodontitis.[7,8]

Pattern recognized receptors (PRRs) play a key role in the host's first line of defense, innate immunity, by detecting conserved microbial components called pathogen-associated molecular patterns (PAMPs).[9] Nucleotide-binding and oligomerization domain (NOD)-like receptors (NLRs) are located in the cytoplasm and consist of an N-terminal effector domain, an intermediate characteristic structure (NACHT), and a C-terminal leucine-rich repeat (LRR).[10]

NLRC5 is the largest protein in the NLR family, which is mostly expressed in immune cells and fibroblasts.[11] NLRC5, originally known as the major histocompatibility complex (MHC) class I transactivator (CITA), plays a critical role in antigen presentation. It has been reported that NLRC5 participates in the occurrence and development of many immune diseases.[12] For example, NLRC5 is involved in inflammatory liver injury and renal inflammation.[13,14] Liu et al. found a potential role of NLRC5 in promoting rheumatoid arthritis progression via the nuclear factor-kappa B (NF-κB) signaling pathway.[15] It has also been reported that a single nucleotide polymorphism of *NLRC5* is related to the susceptibility to chronic periodontitis.[16] However, whether NLRC5 participates in regulatory mechanisms of bone destruction in periodontitis remains unknown. The aim of our study was to demonstrate the regulatory effect of NLRC5 on bone metabolism and to find the relationship between NLRC5 and periodontitis.

In the present study, we found that NLRC5 is expressed in human bone marrow mesenchymal stem cells (hBMSCs) and is upregulated during osteoblast induction. We then overexpressed *NLRC5* in hBMSCs to detect the effect of NLRC5 on osteogenesis. Next, we generated *Nlrc5*-knockout mice to observe the role of NLRC5 in osteogenesis of the femora and alveolar bone resorption caused by experimental periodontitis in vivo. Moreover, in vitro studies were performed to further investigate the effect of NLRC5 on osteoclastogenesis and osteogenesis.

2 | MATERIALS AND METHODS

2.1 | Generation of *Nlrc5*$^{-/-}$ mice and the periodontitis animal model

Nlrc5$^{-/-}$ C57BL/6 mice were generated by Gene Pharma Technology (Nanjing, Jiangsu, China) by deleting the specific sequence: "AATTCTCTAAGCAGCTAGGGGCAGGAGAGGAGAGCTGCCCTGGACCTCAGCTGTA," using clustered regularly interspaced short palindromic repeats (CRISPR)/CRISPR-associated protein 9 (CAS9) technology. *Nlrc5*$^{-/-}$ mice were backcrossed with their parents more than five times to generate homologous *Nlrc5*$^{-/-}$ mice. The *Nlrc5*$^{-/-}$ mice were viable and bred under specific pathogen-free conditions, with no abnormal behavior, in the animal facility of the Peking University Health Center. All animal experiments were performed according to a protocol approved by the Animal Care and Use Committee of Peking University (Code of ethics: 2015106). Genotype identification was performed by extracting DNA from tail tissue and DNA sequencing (Figure S1). Twelve-week-old male mice ($n = 6$ for each group) were chosen to build the periodontitis models to minimize the influence of estrogen. A 5-0 silk thread was soaked in a *P. gingivalis* suspension and ligatured around the second molars in the upper jaw under general anesthetic to induce experimental periodontitis. Then, we inoculated *P. gingivalis* and examined the ligature every other day. Sham-treated mice were used as controls. One week later, the mice were euthanized, and the maxillary tissues were fixed with 4% paraformaldehyde for micro-computed tomography (CT) scanning and histological analysis.

2.2 | Culture and identification of BMSC

The lower limbs of the 4-week-old of WT and NLRC5−/− mice were collected and then the muscles were removed in the super clean table. The femora and tibiae were soaked in 75% alcohol for 15 s and immediately transferred into the α-MEM (Gibco) containing 5% penicillin/streptomycin (Hyclone). Both ends of the femora and tibiae

were cut off with scissors and cells were washed out of them with a 1-milliliter syringe. Then the cells were collected for centrifugation (1000 rpm, 5 min). Cells were resuspended as a single-cell suspension and cultured in 10-cm dishes with α-MEM (Gibco) containing 10% fetal bovine serum and 2% penicillin/streptomycin (Hyclone) in an incubator (full relative humidity, 37°C, 5% CO2) for 48 h. After removing the suspended cells, the adherent cells were continued to culture and the media were changed every 2 days. After the confluence rate closing to 80%–90%, mice bone marrow-derived stem cells (mBMCs) were then passaged and cultured as mBMSCs. mBMSCs were identified by detection of CD34, CD45, CD105, and CD106 using flow cytometry (Figure S2).

Human bone marrow mesenchymal stem cells (hBMSCs) were obtained from ScienCell Co., Ltd.

2.3 | Osteoblast induction, alkaline phosphatase staining, and Alizarin Red S staining

Either hBMSCs or mBMSCs were seeded in 12-well culture plates at a density of 3×10^5 cells per well and allowed to attach overnight. When the cell confluence reached 80%, the BMSCs were cultured in osteogenic medium (OM), which consisted of growth medium supplemented with 10 mmol/L β-glycerophosphate, 0.2 mmol/L ascorbic acid and 100 nmol/L dexamethasone for osteogenic induction. OM was replaced every 3 days.

Alkaline phosphatase (ALP) staining was performed at 14 days after osteoinduction by Alkaline Phosphatase Color Development Kit (#C3206, Beyotime). Cells were washed with phosphate buffered saline (PBS) three times, fixed using 4% paraformaldehyde for 30 min at room temperature, and then stained using a preconfigured working solution consists of 5-bromo-4-chloro-3-indolyl phosphate (BCIP)/nitro blue tetrazolium (NBT). After drying, the plates containing the stained mBMSCs were scanned (#HP Scanjet G4050, Hewlett-Packard) to capture images.

After 21 days induction by OM, calcium nodes were stained with 2% alizarin red S (#A3882, Sigma) according to the manufacturer's instructions. To quantify matrix mineralization, the stained samples were incubated in 10% cetylpyridinium (#C9890, Solarbio) chloride for 1 h to solubilize and release the calcium-bound Alizarin red into the solution. The absorbance of the released Alizarin red was measured using a spectrophotometer (Elx808, BioTek) at 490 nm.

2.4 | Overexpression of *NLRC5* by adenovirus transfection

Adenovirus containing the full-length *NLRC5* cDNA and control vectors were produced by XIEBHC BIO. The cells were plated and allowed to adhere. The next day, human-origin adenovirus transfection medium was prepared, which contained the NLRC5 full-length plasmid with a C-FLAG-tag or control adenoviruses, according to the

appropriate multiplicity of infection (MOI), added to the plate, and cultured for 24 h for further research.

2.5 | Quantitative real-time reverse transcription analysis

Total RNA of cells was extracted from cell lysates using TRIzol (#15596018, Thermo Fisher Scientific) according to manufacturer instructions. The skeletal or gingival tissue of mice were taken and immediately added into thick wall centrifuge tube containing 300-μl TRIzol and a stainless steel ball, then crushed by high flux tissue grinder for 3 min before RNA extraction. The concentration of total RNA was measured by Nanodrop 8000 (Thermo Fisher) and was reverse-transcribed into cDNA with the Prime Script RT master kit (#RR036A, Takara). Quantitative real-time PCR (qPCR) was performed using the ABI 7500 system to quantify the mRNA expression level of the targeted genes. The relative expression level of the mRNA of each gene was evaluated by the $2^{-\Delta \Delta Ct}$ method, relative to the housekeeping gene GAPDH. The primers used are listed in Table S1.

2.6 | Western blotting analysis

Total proteins were extracted using Radio immunoprecipitation assay lysis buffer containing a protease inhibitor cocktail (Sigma) and phosphatase inhibitors (Huaxingbio) to perform western blotting. The protocol of western blotting was described previously.[19] The antibodies used are listed in Table S2.

2.7 | Sampling of human gingival tissue and human gingival fibroblasts

Gingival tissue specimens, and human gingival fibroblasts (hGFs) were obtained as previously described (ethics approval no. PKUSSIRB-201522049).[19] The Protocol of *P. gingivalis* culture and infection were described previously.[29] mRNA expression in gingival tissue and hGFs was detected using Quantitative real-time reverse transcription (qRT-PCR) after TRIzol lysis.

2.8 | X-ray and Micro-CT analyses

The femora were scanned using an Inveon™ Micro-CT instrument (Siemens Medical Solutions) for which the tube voltage and rotation center had been calibrated before use. The parameters were set as follows: Voltage 60 kV, current 220 μA, exposure time 1500 ms, effective pixel value 8.89 μm 360° rotation, every 1° exposure. The region of interest (ROI) was set from 0.8 to 1.3 mm below the growth plate. The data were analyzed with using Inveon Research Workshop software (Siemens Medical Solutions) to

compare the indicators: the ratio of bone volume to total volume (BV/TV), thickness of the trabeculae (Tb.Th), number of trabeculae (Tb. N), and the cortex thickness (Cortex.Th). The severity of alveolar bone resorption by linear measurement evaluation was performed with 2-dimensional and 3-dimensional reconstruction. The ROI was chosen around the second molars and those with the most severe bone absorption. The plane passing through the mesial root canal orifice of the maxillary first molar and the distal root canal orifice of the maxillary second molar, and perpendicular to palatal plane were determined as the evaluation planes (Figure S3). The bone loss height was measured from the cementoenamel junction (CEJ) to the alveolar bone crest at the mesial and distal sites of the second molars. The inspectors were blinded to the grouping when they processed the data.

2.9 | In vivo double labeling with calcein and ARS

Four-week-old mice were injected intraperitoneally with 10 mg/kg 0.05% Calcein (pH = 8.3) on day 0, and with 30 mg/kg 1% Alizarin Red (SARS) (pH = 7.2) on day 7. Mice were sacrificed on day 10, and isolated femora were fixed in 4% paraformaldehyde. Samples were subjected to hard tissue sectioning and fluorescence-labeled images were captured using a laser confocal microscope (LSM700, Zeiss). Under the confocal microscope, calcein showed green fluorescence and ARS showed red fluorescence. The distance between two fluorescent bands was measured using Image-Pro Plus (Media Cybernetics) and the mineral apposition rate (MAR) was calculated by dividing the distance by days to represent the bone-formation activity (unit: μm/d).

2.10 | Histological and radiological evaluation

The fixed maxillary tissues were decalcified for 2 weeks using 10% EDTA decalcification solution. After dehydration, the tissues were embedded in wax and cut into sections for hematoxylin and eosin (HE) staining and TRAP staining. Images were captured under an optical microscope. The age-matched wild-type (WT) mice served as the control.

2.11 | Osteoclast induction, TRAP assay and Pit-absorption assay

The spleens were collected from 4-week-old WT and $Nlrc5^{-/-}$ mice to culture primary splenocytes. Splenocytes were cultured in osteoclast induction medium (OM) (α-MEM + 10% FBS + 1% penicillin–streptomycin + 30 ng/ml RANKL + 100 ng/ml macrophage colony stimulating factor [M-CSF]) to induce the differentiation of osteoclasts. The control group was cultured in proliferation media (PM) containing only 10% FBS and 1% penicillin–streptomycin. On the 5th day, the cells were collected to extract total protein and RNA.

After the cells were fixed, TRAP staining was performed using a TRAP staining kit (Sigma), according to the manufacturer's instructions. After staining with the dye solution at 37°C for 1 h, the samples were rinsed and observed under a microscope.

The primary splenocytes from the mice were inoculated onto Osteo Assay Surface 24-well culture plates at a density of 3×10^5 cells per well and induced by OM for 7 days. Then the cells were soaked in 10% sodium hypochlorite solution for 5 min, washed three times with distilled water, and dried. The bone-resorption area was observed and photographed under an inverted microscope, and the ratio of the bone-resorption area was calculated using Image-Pro Plus software.

2.12 | Statistical analysis

Statistical analysis was performed using SPSS 20.0 software (IBM Corp.). All data are presented as the mean ± SD. Statistically significant differences were assessed using one-way analysis of variance (ANOVA) and Newman–Keuls post hoc tests. A value of $p < .05$ was considered to be statistically significant. All the experiments were repeated more than three times.

3 | RESULTS

3.1 | Overexpression of *NLRC5* stimulated bone formation and mineralization

Initially, hBMSCs were cultured in OM for 14 days to induce osteogenesis. After induction for 3 and 5 days, the expression of *NLRC5* was upregulated (Figure 1A). To identify the role of NLRC5 in the process of osteoblast induction, hBMSCs were induced with OM after infection with adv-NLRC5 (Figure 1B). The ALP staining showed that the number of osteoblast-like cells increased in response to NLRC5 overexpression (Figure 1C). The quantification of ARS staining showed that overexpression of *NLRC5* increased the number of mineralized nodules and enhanced the cells' mineralization ability (Figure 1D).

Cells infected with adv-NLRC5 were harvested and subjected to total RNA extraction. qRT-PCR showed that overexpression of *NLRC5* led to increased expression of the mRNA encoding osteogenic biomarkers, including the transcription factors RUNX2 and Osterix (OSX), as well as the osteoblast markers ALP and osteocalcin (OCN) (Figure 1E).

3.2 | *Nlrc5*$^{-/-}$ mice have fewer bone trabeculae than WT mice at early age

$Nlrc5^{-/-}$ mice were constructed using CRISPR/Cas9 technology to examine the effect of NLRC5 on bone development. We collected the femora from 6-week-old mice and performed histological
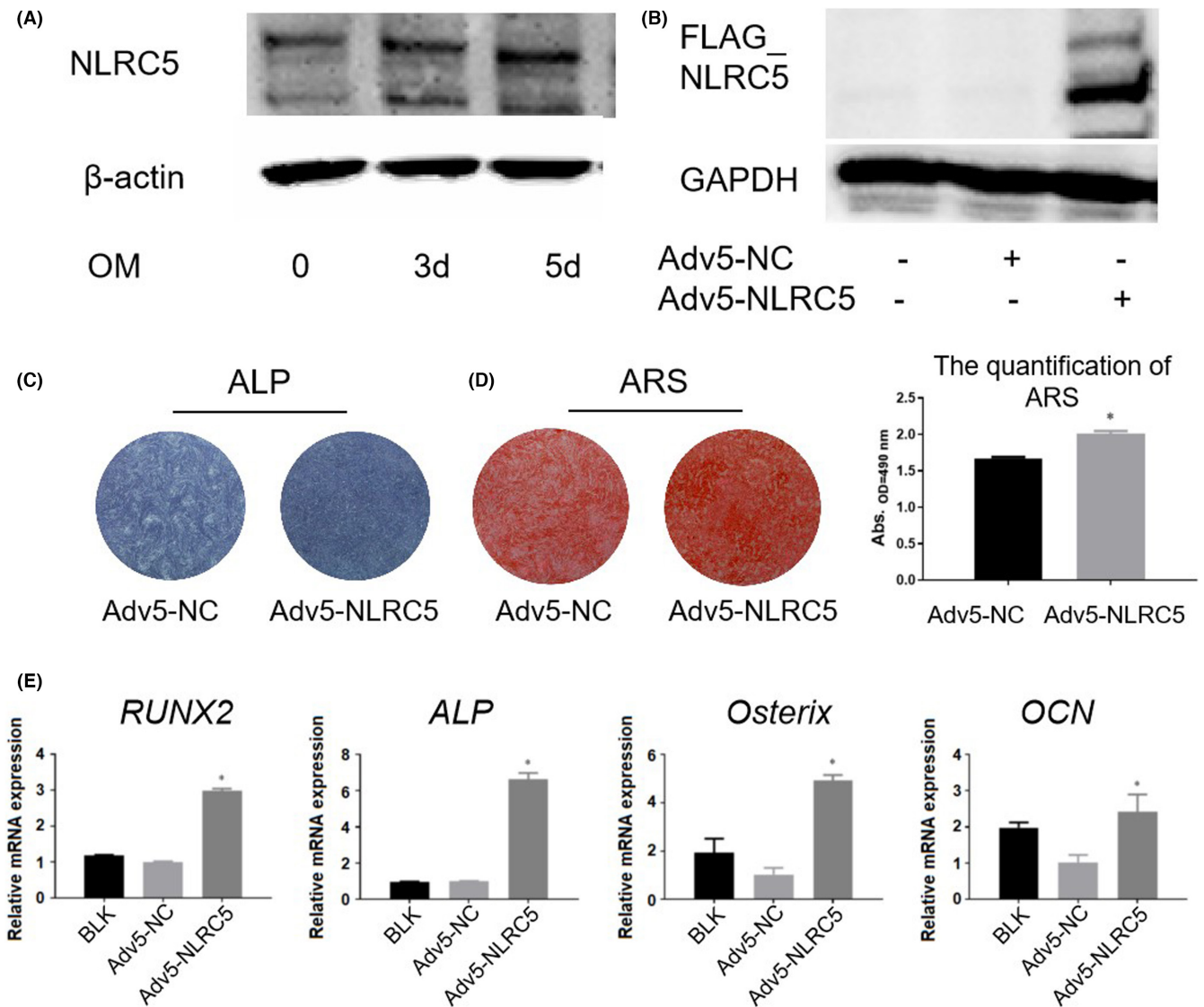
FIGURE 1 Bone formation and mineralization after NLRC5 overexpression in hBMSCs by adenovirus infection. (A) NLRC5 expression at day 3 and day 5 during OM induction. (B) NLRC5 overexpression by adenovirus infection was identified using western blotting. (C) ALP staining after OM induction. (D) ARS staining assay of mineral nodes. The quantification of mineral nodes by ARS staining after OM induction for 21 days (*$p < .05$). (E) The mRNA levels of *RUNX2*, *ALP*, *Osterix*, and *OCN* were detected using qRT-PCR (*$p < .05$). NLRC5, NOD-like receptor; hBMSCs, human bone marrow mesenchymal stem cells; OM, osteogenic medium; ALP, alkaline phosphatase; ARS, Alizarin Red S; RUNX2, Runt-related transcription factor 2; OCN, Osteocalcin; qRT-PCR, quantitative real-time reverse transcription PCR.

examinations. Hematoxylin and eosin (HE) staining assay and Masson staining assays showed that the $Nlrc5^{-/-}$ group had fewer bone trabeculae below the growth plate (Figure 2A and B). At the same level below the growth palate, the bone cortex was thinner in the $Nlrc5^{-/-}$ group compared with that in the WT group. The trabecular area per unit was calculated using Image-Pro plus. The area in the $Nlrc5^{-/-}$ group was significantly smaller than that in the WT group (Figure 2C).

To further verify the influence of NLRC5 on bone trabeculae and bone cortex, we collected the femora and scanned them using micro-CT. The 3-D reconstruction images suggested that the quality and quantity of the trabeculae were reduced in the $Nlrc5^{-/-}$ group

compared with those in the WT group (Figure 2D). The bone volume and the number trabeculae were significantly lower in the $Nlrc5^{-/-}$ group than in the WT group, while the thickness of trabeculae and the ratio of bone volume and total volume also decreased by $Nlrc5$ knockout without statistical difference (Figure 2E). These results showed that $Nlrc5$ knockout affected the quantity of trabecular bone. The cortex thickness measured at the horizontal level in the $Nlrc5^{-/-}$ group was markedly more spaced out than that in the WT group (Figure 2F). All the radiographical results suggested that $Nlrc5$ knockout affected the quality of the trabeculae and the cortex. The difference in trabecular and cortex of the femora were significant before the age of 8 weeks and gradually eliminated until 12 weeks (data not shown).

(A) HE

(B) Masson Staining

(C)

(D) 3D reconstruction

(E)

(F) 2D measurement
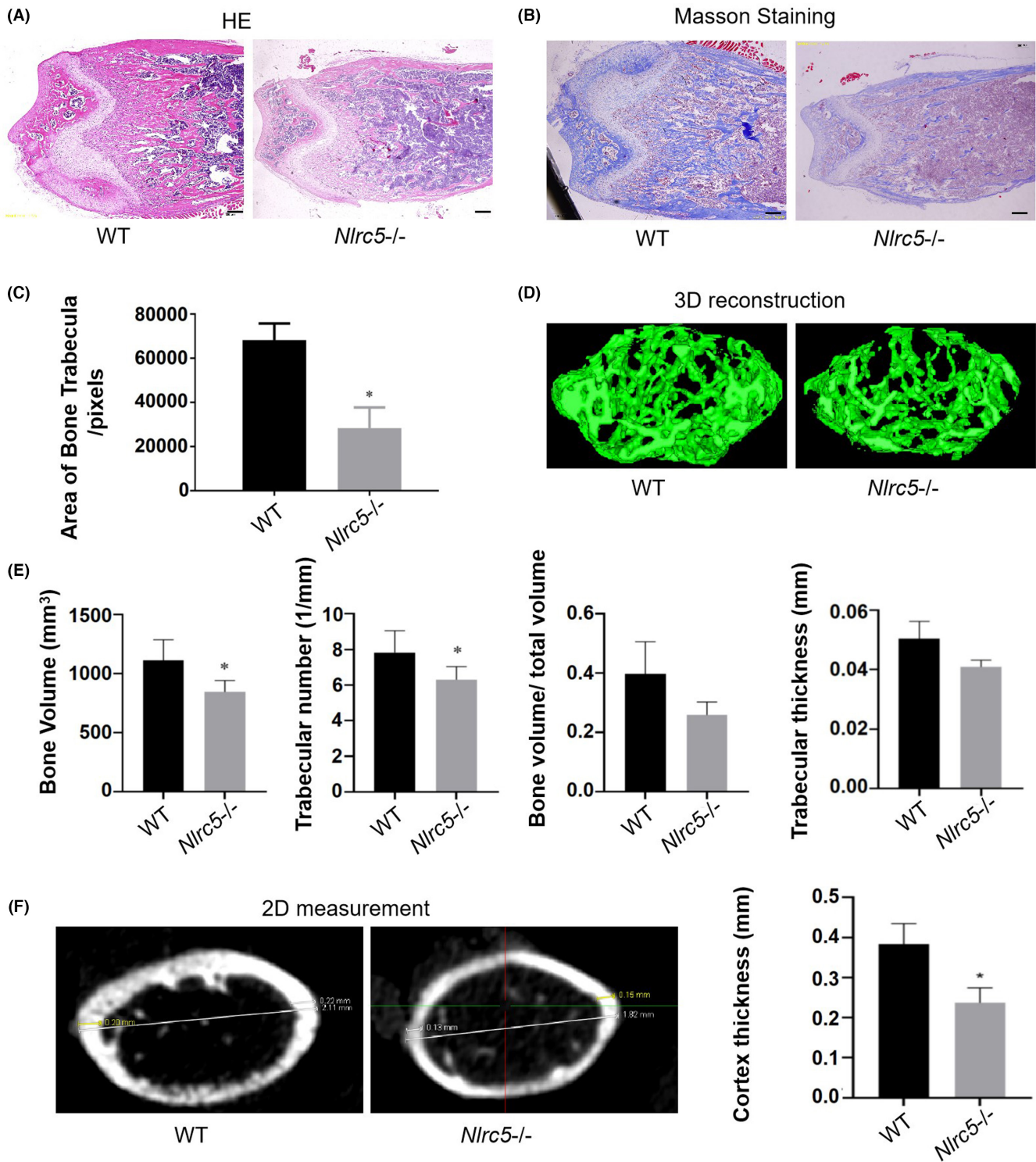
FIGURE 2 Trabeculae of the femora were loose and sparse in the *Nlrc5*-knockout mice group. (A) HE staining assay showed that the trabeculae of femora below the growth plate were loosened in the *Nlrc5*-knockout group. (B) Modified Masson staining assay showed that the trabeculae of the femora below the growth plate were loosened in the *Nlrc5*-knockout group. (C) The area of bone trabeculae was significantly reduced in the *Nlrc5*-knockout group (*$p < .05$). (D) 3Dimensional (3D) reconstruction images of the femora from the wild-type (WT) and *Nlrc5*−/− groups. (E) The femora from the WT and *Nlrc5*−/− groups were compared at the level of bone volume, the number of trabeculae (Tb.N), the ratio of bone volume to total volume (BV/TV), and thickness of the trabeculae (Tb.Th) (*$p < .05$). (F) The cortex thickness (Th.cortex) of the femora in the WT and *Nlrc5*−/− group were measured in 2Dimensional (2D) axial images from the horizontal level (*$p < .05$). NLRC5, NOD-like receptor; HE, hematoxylin and eosin.

3.3 | Reduced bone mineralization by *Nlrc5* knockout

To determine the influence of NLRC5 on bone formation and development, we collected the femora from the mice and made hard tissue sections. The sections were observed under a laser confocal microscope. Calcein showed green fluorescence and ARS showed red fluorescence. The view near the growth plate was regarded as the ROI. The region was captured and the distance between the two fluorescent lines was measured. Fluorescent images showed that the distance between the lines in the *Nlrc5*-knockout group was much shorter than that of the WT (Figure 3A). The mineralized apposition rate (MAR) was calculated using the distance between the two fluorescent lines divided by the number of days. The MAR in the $Nlrc5^{-/-}$ group was 2.52 μm/day, while that in the WT group was 3.61 μm/day (Figure 3B). These results suggested that the osteogenic ability was significantly weakened after depletion of NLRC5.

After proteins were extracted from mBMSCs from $Nlrc5^{-/-}$ and WT mice, western blotting confirmed the NLRC5 protein level in both groups (Figure 3C). ALP and ARS assays showed that *Nlrc5* knockout led to decreased osteogenesis in mBMSCs compared with that in WT cells (Figure 3D,E). The mRNA expression levels of *Runx2*, *Alp*, *Osx*, and *Ocn*, which are osteogenic biomarkers, in mBMSCs and skeletal tissue, were downregulated in the $Nlrc5^{-/-}$ group (Figure 3F).

3.4 | Increased osteoclast activity was observed after *Nlrc5* knockout

Bone remodeling is dependent on osteoclasts absorbing the old bone and osteoblasts depositing new mineralized materials to form new bone. To further elucidate the impact of NLRC5 on osteoclastogenesis, splenocytes were extracted from both groups as pre-osteoclasts. The osteoclasts were induced by 20 ng/mL RANKL and 30 ng/mL M-CSF for 7 days and identified by TRAP staining. The results showed that the cell volume of the osteoclasts, rather than number of osteoclasts, in the $Nlrc5^{-/-}$ group was obviously increased (Figure 4A). Pit-absorption assays also showed that the destruction in the $Nlrc5^{-/-}$ group was enhanced (Figure 4B). Moreover, the qRT-PCR results showed the expression levels of *Trap*, *Ctsk* (cathepsin K), *Dc-stamp*, and *Mmp9*, which are osteoclasts indicators, were higher in the $Nlrc5^{-/-}$ group after the induction of osteoclasts (Figure 4C).

3.5 | Upregulation of NLRC5 was identified in *P. gingivalis* challenged hGFs and periodontitis patient

The above experimental results proved that NLRC5 has the ability to regulate non-inflammatory bone metabolism. As a member of the pattern recognition receptor family, it is of great significance to study whether NLRC5 can play a role in inflammatory bone-resorption diseases.

Compared with healthy controls, the expression of *NLRC5* decreased significantly in gingival tissue of patients with periodontitis (Figure 5A). After hGFs were challenged by a putative periodontal pathogen, *P. gingivalis*, for 2, 4, and 8 h, a downregulation of NLRC5 expression was verified by qRT-PCR and western blotting (Figure 5B and C).

3.6 | Increased bone destruction and severe inflammation were observed in $Nlrc5^{-/-}$ periodontitis model mice

To further investigate the effect of NLRC5 on periodontal bone resorption, micro-CT scans were performed on alveolar bone from a periodontitis model induced by ligature and *P. gingivalis* infection. 12-week old male mice were selected to minimize the influence of estrogen and the difference of bone mineral density at baseline. More bone destruction was observed in the $Nlrc5^{-/-}$ group than in the WT group (Figure 5D). Linear analysis of bone loss by 2D section images also showed worse bone loss in the $Nlrc5^{-/-}$ group (Figure 5E and F). TRAP staining showed more osteoclasts in the $Nlrc5^{-/-}$ group than in the WT group (Figure 5G). Meanwhile, more inflammatory cell infiltration were observed in $Nlrc5^{-/-}$ group by HE staining and labeling leukocyte common antigen (LCA, CD45$^+$) (Figure 6A,B). Except for IL-8, the expression of IL-1β, IL-6, and TNF-α at mRNA level in gingival tissue were increased more significantly in the $Nlrc5^{-/-}$ group than in the WT group (Figure 6C).

4 | DISCUSSION

It has been demonstrated that besides participating in the immune response, several PRRs are closely related to bone metabolism. Poly(I:C) and CpG ODN C, as the ligands of Toll like receptor (TLR)3 and TLR9, were reported to have potential applications as immunomodulators of bone regeneration.[17] The MHC class II transactivator (CIITA) was found to be a positive regulator of osteoclast differentiation and bone resorption.[18] In this study, we demonstrated a novel and non-immune function of NLRC5 in the regulation of bone metabolism. The $Nlrc5^{-/-}$ mice showed a phenotype of decreased osteogenic ability in the femora and in vitro findings revealed that NLRC5 is a positive regulator of osteogenesis and a negative regulator of osteoclastogenesis. However, the difference in bone mineralization only exists in the process of growth and development. It means that with the increasing age, some other regulatory factors in the whole body could compensate for the inhibitory effect of NLRC5 knock out on bone development. Considering the multiple functions of NLRC5, the major organs including the heart, liver, spleen, and kidney were sectioned for HE staining. The result showed no evident pathological changes in the major organs in the $Nlrc5^{-/-}$ mice (Figure S4). The mechanism by which NLRC5 regulates bone growth and body self-repair require further study.
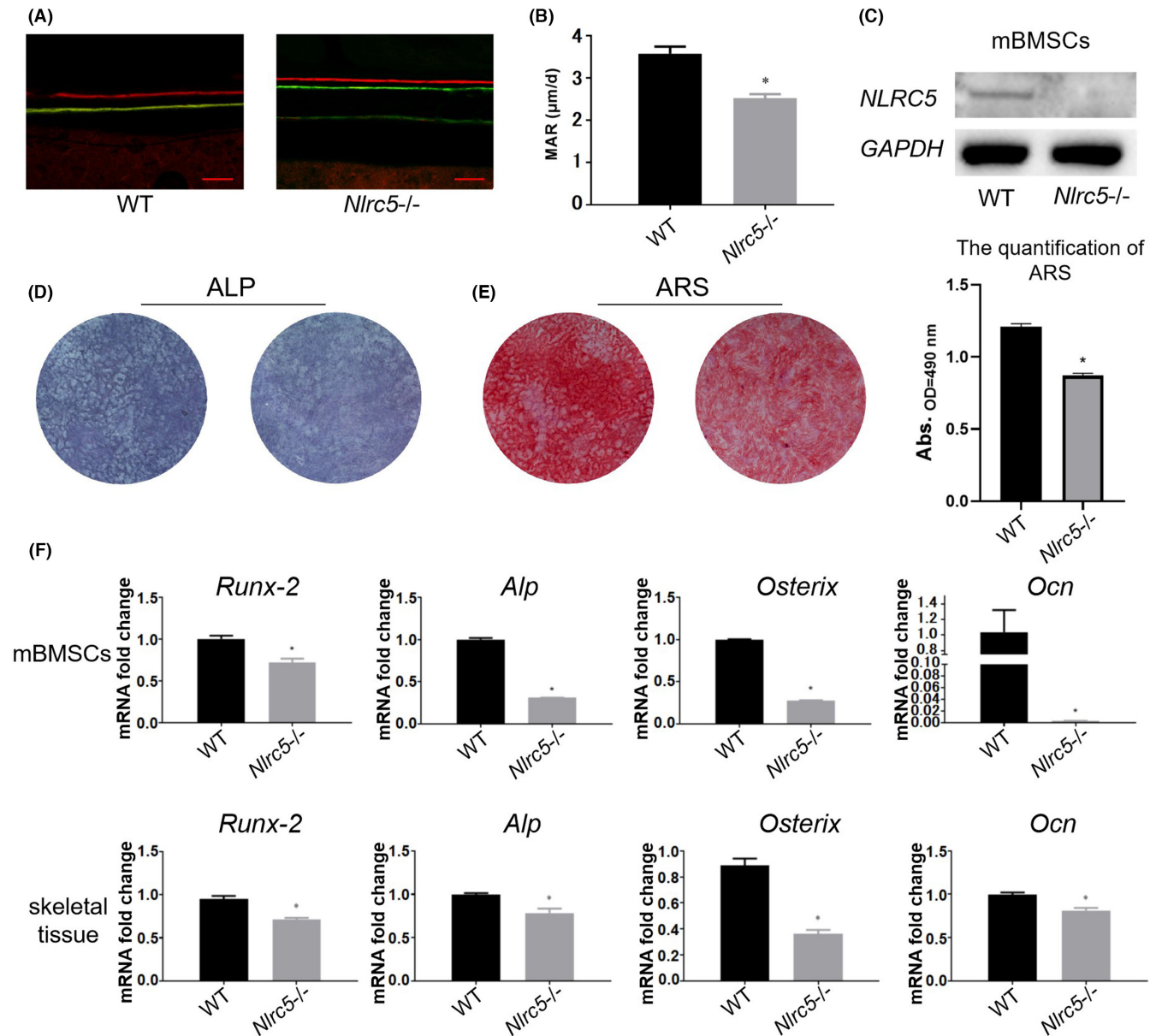
FIGURE 3 Osteogenic ability of mice was weakened in the $Nlrc5^{-/-}$ group. (A) Fluorescent images were captured by laser confocal microscopy (green fluorescence represents the position of calcein and red fluorescence represents ARS staining, the distance between two fluorescent lines represents mineralized deposition over 7 days; the red scale is 100 μm). (B) The mineralized apposition rate (MAR) was calculated by the distance between the two fluorescent lines divided by the number of days. MAR was used to represent the activity of osteoblasts and the osteogenic ability ($*p < .05$). (C) $Nlrc5$ expression in mBMSCs from WT group and $Nlrc5^{-/-}$ group. (D) ALP staining after OM induction. (E) ARS staining of mineral nodes. The quantification of mineral nodes by ARS staining after OM induction for 21 days ($*p < .05$). (F) The mRNA levels of $RUNX-2$, ALP, $Osterix$, and OCN in mBMSCs and skeltal tissue ($*p < .05$). NLRC5, NOD-like receptor; mBMSCs, mouse bone marrow mesenchymal stem cells; OM, osteogenic medium; ALP, alkaline phosphatase; ARS, Alizarin Red S; RUNX-2, Runt-related transcription factor 2; OCN, Osteocalcin; qRT-PCR, quantitative real-time reverse transcription PCR.

Periodontitis is a chronic infectious disease with periodontal tissue destruction initiated by pathogenic microorganisms. Accumulating evidence has demonstrated dysregulated inflammatory responses activated by PRRs, leading to the release of multiple cytokines associated with bone metabolism, which ultimately favors the destruction of the periodontium.[19–21] NLR family pyrin domain containing 12 (NLRP12) attenuated bone loss in experimental apical periodontitis.[22] *Porphyromonas gingivalis*-induced

periodontal bone resorption in mice was found to be dependent on TLR4.[23] Other researchers have found that nucleotide-binding oligomerization domain containing 2 (NOD2) promotes *P. gingivalis*-induced bone resorption, whereas no difference in the number of TRAP-positive cells was observed.[24] NLRC5 can exert different functions in various immune diseases dependent on the cell types, via various signaling networks. Combined with the above research results, NLRC5 might be a bridge between the immune system and

FIGURE 4 Osteoclast induction of primary splenocytes by RANKL and M-CSF. (A) The osteoclasts identified by TRAP staining after osteoclast induction of splenocyte-derived mononuclear cells. The black scale is 100 μm. (B) The area of pit absorption were calculated after osteoclast induction of splenocytes (*p < .05). The yellow scale is 500 μm. (C) The mRNA level of *TRAP, CTSK, DC-Stamp*, and *MMP9* were measured using qRT-PCR (*p < .05). RANKL, receptor activator of nuclear factor-kappa B ligand; M-CSF, macrophage colony stimulating factor; TRAP, Tartrate-resistant acid phosphatase; CTSK; cathepsin K, DC-STAMP, dendrocyte expressed seven transmembrane protein; MMP, matrix metalloproteinase; qRT-PCR, quantitative real-time reverse transcription PCR.
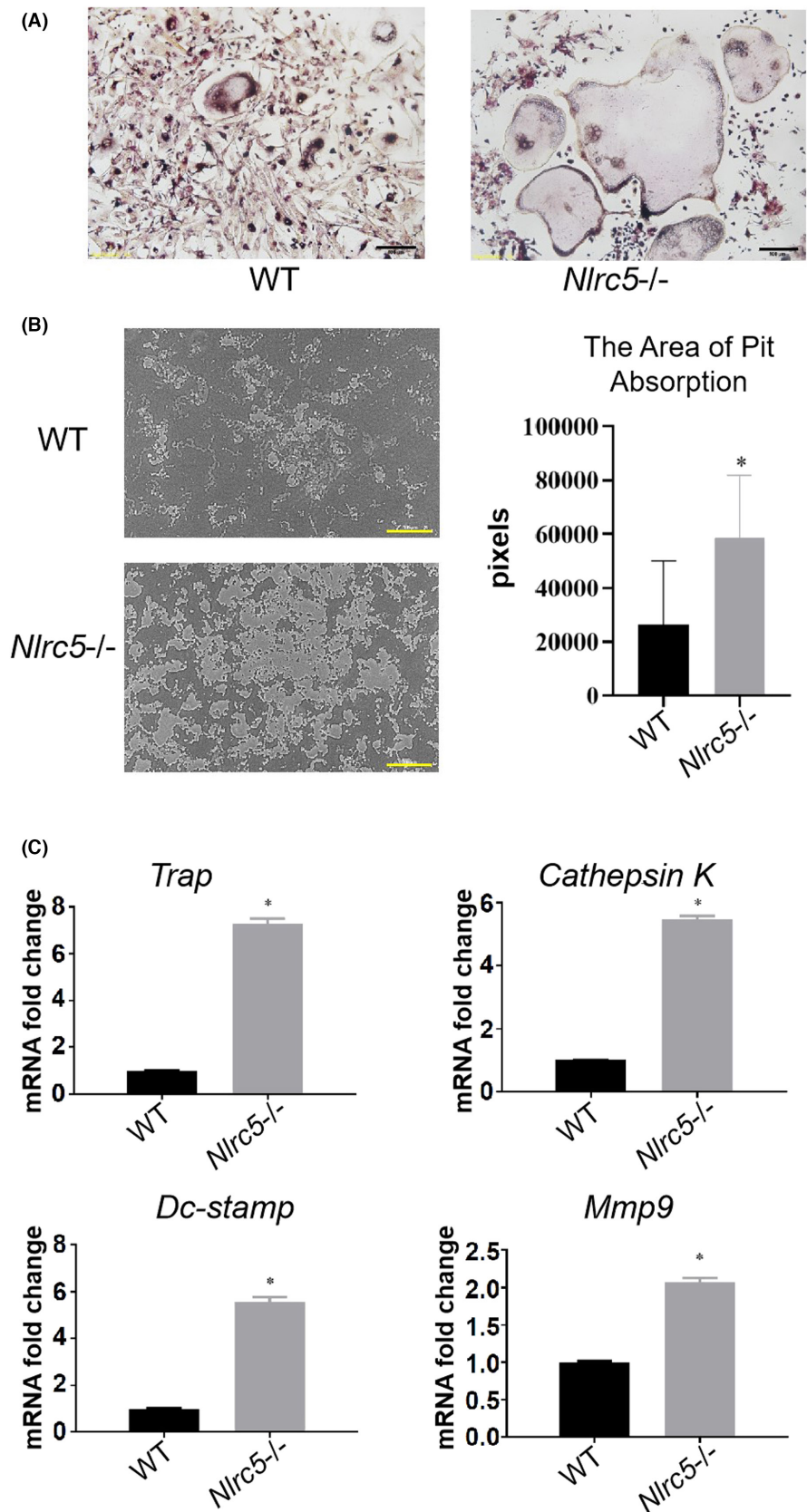
bone homeostasis. In this study, more alveolar bone resorption was observed in the *Nlrc5*⁻/⁻ mice compared with that in the WT mice in experimental periodontitis. Unlike other PRRs previously found to promote periodontitis, NLRC5 is identified to have a potent protective role in inflammatory periodontal bone loss for the first time.
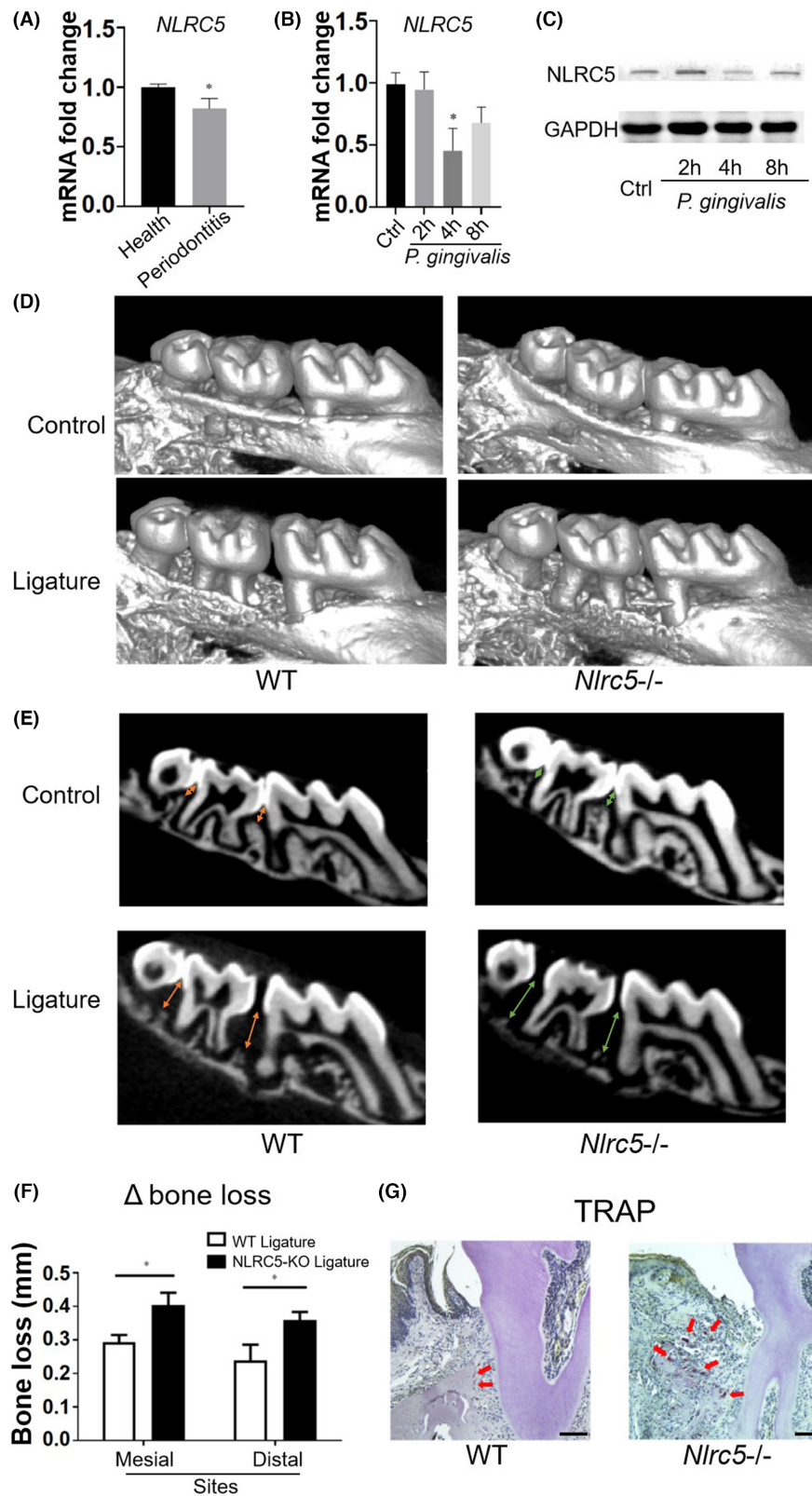
FIGURE 5 NLRC5 is involved in periodontitis and negatively regulates alveolar bone loss. (A) *NLRC5* mRNA expression in the periodontitis group and healthy group. (B) *NLRC5* expression in hGFs after *Porphyromonas gingivalis* challenge for 2, 4, and 8 h at mRNA level. (C) NLRC5 expression in in hGFs after *P. gingivalis* challenge for 2, 4, and 8 h at protein level. (D) 3D image showed the distance from cementoenamel junction (CEJ) to the alveolar bone crest. E Image of 2Dimensional (2D) sections showed alveolar bone resorption. (F) The linear bone destruction in the mesial and distal sides of the second molar in the maxillary (*$p < .05$). (G) Osteoclasts (red arrow) were detected by TRAP staining in sections of the maxillary. The black scale is 50 μm. NLRC5, NOD-like receptor; hGFs, human gingival fibroblast; qRT-PCR, quantitative real-time reverse transcription PCR; TRAP, Tartrate-resistant acid phosphatase.

Although specific ligands of NLRC5 have not been confirmed, bacteria, such *Escherichia coli* and *Helicobacter pylori*, or virulence factors, such as lipopolysaccharide, have been reported to affect the expression of NLRC5.[25–27] It has also been reported that lipoteichoic acid activates NLRC5 via TLR2/NF-κB.[28] *Porphyromonas gingivalis* is one of the most important pathogenic bacteria and it is recognized by several NLRs.[29,30] However, we found that *P. gingivalis* infection decreased NLRC5 expression at both cell and tissue level. Moreover, in the model of experimental periodontitis induced by ligature and *P. gingivalis* infection, *Nlrc5*^{−/−} group exhibited more inflammatory cell
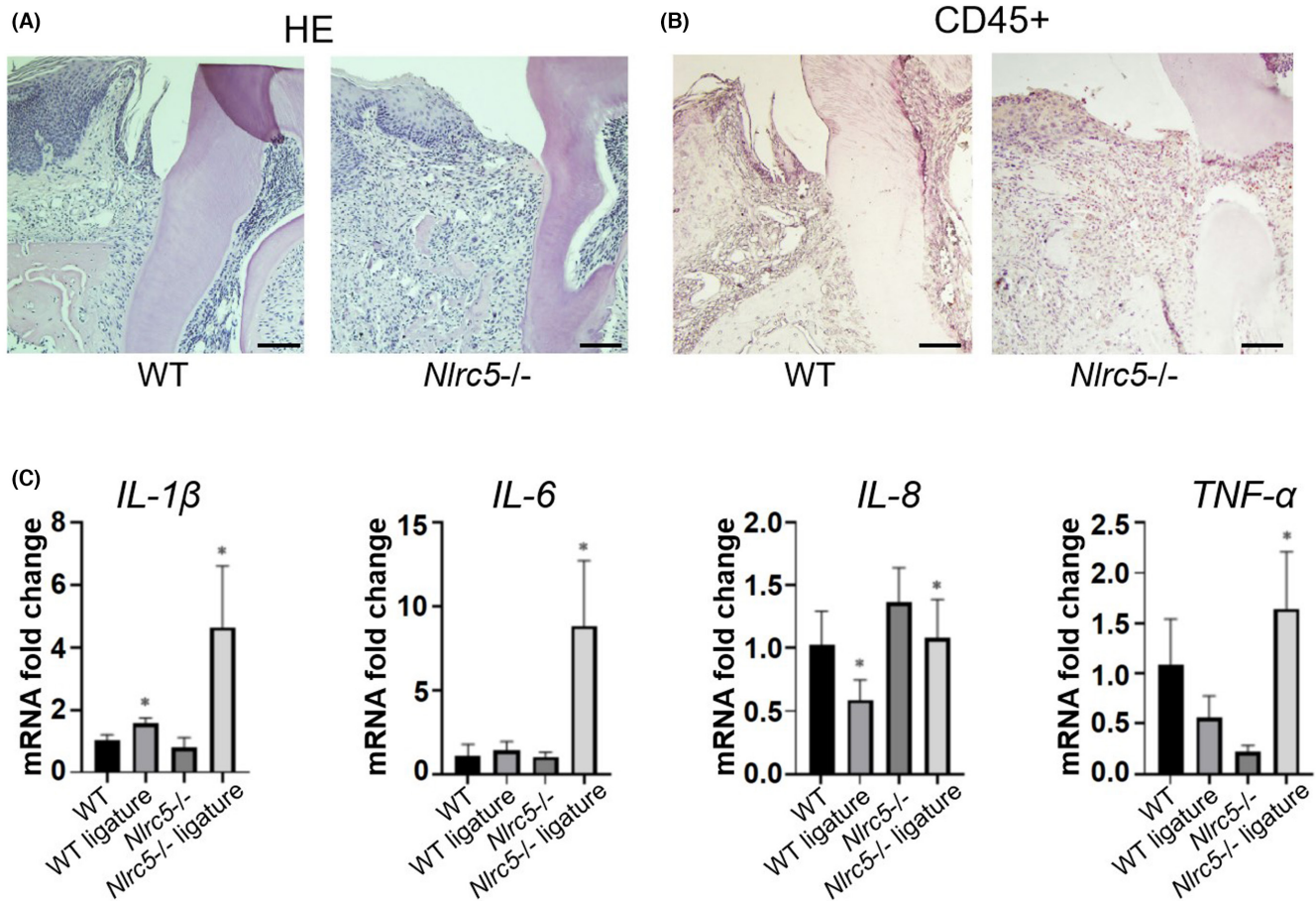
FIGURE 6 Increased inflammation in $Nlrc5^{-/-}$ mice with periodontitis. (A) Inflammatory infiltrating cells in the gingiva were observed using HE staining. The black scale is 50 μm. (B) CD45$^+$ cells in the gingiva were determined by IHC assay. The black scale is 50 μm. C The mRNA level of *IL-1β*, *IL-6*, *IL-8*, and *TNF-a* were measured using qRT-PCR (*$p < .05$). NLRC5, NOD-like receptor; HE, hematoxylin and eosin; CD45, cluster of differentiation 45; IHC, immunohistochemistry; IL, interleukin; TNF-α, tumor necrosis factor alpha; qRT-PCR, quantitative real-time reverse transcription PCR.

infiltration and inflammatory cytokines secretion than WT group. IL-1β, IL-6, and TNF-α also have the ability to activate and differentiate osteoclasts by diverse inflammatory signaling pathways.[31,32] We also noticed that the expression of IL-8, a chemokine associated with granulocyte accumulation, is decreased after ligatured. It might implicate that the inflammatory cell infiltration activity is static while the alveolar bone resorption is established in the animal model. Dysregulation of inflammatory responses could break the balance of osteoblasts and osteoclasts, resulting in alveolar bone resorption. The upregulation of those cytokines in the gingiva from $Nlrc5^{-/-}$ mice could be another reason for the accelerated alveolar bone resorption beyond directly modulating bone metabolism.

Although the above evidence points to NLRC5 being a negative regulator of periodontitis, the difference in alveolar bone resorption was significant, but mild. Recent studies have revealed multiple but contradictory roles of NLRC5 in different inflammatory responses. NLRC5, originally known as CITA, plays a critical role in antigen presentation and major histocompatibility complex (MHC) class I transcription.[33] The expression of MHC-I like molecule CD1d was found to be more frequent in periodontitis

and increased in parallel with invariant natural killer T cell infiltration.[34] According research by Benko et al., knockdown of *Nlrc5* in RAW 264.7 cells (a mouse macrophage cell line) increased the secretion of the proinflammatory cytokines in response to interferon gamma (IFN-γ) and lipopolysaccharide, including TNF, IL-6, and IL-1β.[12] Overexpression of *Nlrc5/NLRC5* in RAW 264.7 and HEK-293 T cells leads to negative regulation of inflammatory pathways.[12] Nevertheless, several studies have implicated NLRC5 in the positively regulation of the NF-κB pathway.[35,36] NLRC5 could even enhance IL-6 and IL-1β secretion by LX-2 cells and the activity of the NF-κB/Smad3 pathway.[35] The Wnt/β-catenin signaling pathway is important in osteogenic differentiation and the accumulation of mineralization. Peng et al. found that NLRC5 could interact with Wnt/β-catenin in hepatocellular carcinoma.[37] In this experiment, since a systemic gene knockout of *Nlrc5* was carried out, there could be several factors in vivo that simultaneously regulate bone homeostasis. Considering these contradictory results, the signaling pathways involved in the regulation of periodontal bone metabolism by NLRC5 need to be further investigated and carefully interpreted.

In conclusion, our results suggested that NLRC5 not only plays a critical role in the differentiation and activity of both osteoclasts and osteoblasts, but also participates in the regulation of periodontal inflammation. These findings indicate a new mechanism in the pathogenesis of periodontitis, and NLRC5 can be considered a potential target for the prevention and treatment of periodontitis or other bone-wasting diseases.

AUTHOR CONTRIBUTIONS

W. Wang and W. Liu contributed to design of experiment; data acquisition, analysis, and interpretation; drafted the manuscript; critically revised the manuscript; gave final approval; and agreed to be accountable for all aspects of work. J. Liu and P. Lv contributed to data acquisition, analysis, and interpretation. Gave final approval; Y. Wang and X. Ouyang contributed to conception and design and agreed to be accountable for all aspects of work.

ACKNOWLEDGMENT

DATA AVAILABILITY STATEMENT

The data that support the findings of this study are available from the corresponding author upon reasonable request.

REFERENCES

1. Nakashima K, de Crombrugghe B. Transcriptional mechanisms in osteoblast differentiation and bone formation. *Trends Genet*. 2003;19(8):458-466.
2. Sims NA, Martin TJ. Osteoclasts provide coupling signals to osteoblast lineage cells through multiple mechanisms. *Annu Rev Physiol*. 2020;82:507-529.
3. Teitelbaum SL. Bone resorption by osteoclasts. *Science*. 2000;289(5484):1504-1508.
4. Vignery A. Macrophage fusion: the making of osteoclasts and giant cells. *J Exp Med*. 2005;202(3):337-340.
5. Yagi M, Miyamoto T, Toyama Y, Suda T. Role of DC-STAMP in cellular fusion of osteoclasts and macrophage giant cells. *J Bone Miner Metab*. 2006;24(5):355-358.
6. Pihlstrom BL, Michalowicz BS, Johnson NW. Periodontal diseases. *The Lancet*. 2005;366(9499):1809-1820.
7. Rho J, Takami M, Choi Y. Osteoimmunology: interactions of the immune and skeletal systems. *Mol Cells*. 2004;17(1):1-9.
8. Takayanagi H. Osteoimmunology: shared mechanisms and crosstalk between the immune and bone systems. *Nat Rev Immunol*. 2007;7(4):292-304.
9. Takeuchi O, Akira S. Pattern recognition receptors and inflammation. *Cell*. 2010;140(6):805-820.
10. Jeong E, Lee JY. Intrinsic and extrinsic regulation of innate immune receptors. *Yonsei Med J*. 2011;52(3):379-392.
11. Meissner TB, Li A, Kobayashi KS. NLRC5: a newly discovered MHC class I transactivator (CITA). *Microbes Infect*. 2012;14(6):477-484.
12. Benko S, Magalhaes JG, Philpott DJ, Girardin SE. NLRC5 limits the activation of inflammatory pathways. *J Immunol*. 2010;185(3):1681-1691.
13. Chen Z, Ding T, Ma CG. Dexmedetomidine (DEX) protects against hepatic ischemia/reperfusion (I/R) injury by suppressing inflammation and oxidative stress in NLRC5 deficient mice. *Biochem Biophys Res Commun*. 2017;493(2):1143-1150.
14. Han F, Gao Y, Ding CG, et al. Knockdown of NLRC5 attenuates renal I/R injury in vitro through the activation of PI3K/Akt signaling pathway. *Biomed Pharmacother*. 2018;103:222-227.
15. Liu YR, Yang L, Xu QQ, et al. Long noncoding RNA MEG3 regulates rheumatoid arthritis by targeting NLRC5. *J Cell Physiol*. 2019;234(8):14270-14284.
16. Zupin L, Navarra CO, Robino A, et al. NLRC5 polymorphism is associated with susceptibility to chronic periodontitis. *Immunobiology*. 2017;222(5):704-708.
17. Khokhani P, Rahmani N, Kok A, et al. Use of Therapeutic Pathogen Recognition Receptor Ligands for Osteo-Immunomodulation. *Materials (Basel, Switzerland)*. 2021;14(5):1119-1133.
18. Benasciutti E, Mariani E, Oliva L, et al. MHC class II transactivator is an in vivo regulator of osteoclast differentiation and bone homeostasis co-opted from adaptive immunity. *J Bone Miner Res*. 2014;29(2):290-303.
19. Liu J, Duan J, Wang Y, Ouyang X. Intracellular adhesion molecule-1 is regulated by *Porphyromonas gingivalis* through nucleotide binding oligomerization domain-containing proteins 1 and 2 molecules in periodontal fibroblasts. *J Periodontol*. 2014;85(2):358-368.
20. Wan M, Liu J, Ouyang X. Nucleotide-binding oligomerization domain 1 regulates *Porphyromonas gingivalis*-induced vascular cell adhesion molecule 1 and intercellular adhesion molecule 1 expression in endothelial cells through NF-kappaB pathway. *J Periodontal Res*. 2015;50(2):189-196.
21. Liu W, Liu J, Wang W, Wang Y, Ouyang X. NLRP6 induces pyroptosis by activation of caspase-1 in gingival fibroblasts. *J Dent Res*. 2018;97(12):1391-1398.
22. Taira TM, Lima V, Prado DS, et al. NLRP12 attenuates inflammatory bone loss in experimental apical periodontitis. *J Dent Res*. 2019;98(4):476-484.
23. Lin M, Hu Y, Wang Y, et al. Different engagement of TLR2 and TLR4 in *Porphyromonas gingivalis* vs. ligature-induced periodontal bone loss. *Braz Oral Res*. 2017;31:e63.
24. Prates TP, Taira TM, Holanda MC, et al. NOD2 contributes to *Porphyromonas gingivalis*-induced bone resorption. *J Dent Res*. 2014;93(11):1155-1162.
25. Marth CD, Firestone SM, Glenton LY, Browning GF, Young ND, Krekeler N. Oestrous cycle-dependent equine uterine immune response to induced infectious endometritis. *Vet Res*. 2016;47(1):110.
26. Chonwerawong M, Ferrand J, Chaudhry HM, et al. Innate immune molecule NLRC5 protects mice from Helicobacter-induced formation of gastric lymphoid tissue. *Gastroenterology*. 2020;159(1):169-182.e8.
27. Fan GW, Zhang Y, Jiang X, et al. Anti-inflammatory activity of baicalein in LPS-stimulated RAW264.7 macrophages via estrogen receptor and NF-kappaB-dependent pathways. *Inflammation*. 2013;36(6):1584-1591.
28. Wang M, Wang L, Fang L, Li S, Liu R. NLRC5 negatively regulates LTA-induced inflammation via TLR2/NF-kappaB and participates in TLR2-mediated allergic airway inflammation. *J Cell Physiol*. 2019;234(11):19990-20001.
29. Wan M, Liu JR, Wu D, Chi XP, Ouyang XY. E-selectin expression induced by *Porphyromonas gingivalis* in human endothelial cells via nucleotide-binding oligomerization domain-like receptors and Toll-like receptors. *Mol Oral Microbiol*. 2015;30(5):399-410.
30. Groeger S, Meyle J. Oral mucosal epithelial cells. *Front Immunol*. 2019;10:208.
31. Kusano K, Miyaura C, Inada M, et al. Regulation of matrix metalloproteinases (MMP-2, −3, −9, and −13) by interleukin-1 and interleukin-6 in mouse calvaria: association of MMP induction with bone resorption. *Endocrinology*. 1998;139(3):1338-1345.

32. Zhao B. TNF and Bone Remodeling. *Curr Osteoporos Rep*. 2017;15(3):126-134.

33. Kobayashi KS, van den Elsen PJ. NLRC5: a key regulator of MHC class I-dependent immune responses. *Nat Rev Immunol*. 2012;12(12):813-820.

34. Amanuma R, Nakajima T, Yoshie H, Yamazaki K. Increased infiltration of CD1d and natural killer T cells in periodontal disease tissues. *J Periodontal Res*. 2006;41(1):73-79.

35. Xu T, Ni MM, Huang C, et al. NLRC5 Mediates IL-6 and IL-1beta Secretion in LX-2 Cells and Modulated by the NF-kappaB/Smad3 Pathway. *Inflammation*. 2015;38(5):1794-1804.

36. Liu X, Wu Y, Yang Y, et al. Role of NLRC5 in progression and reversal of hepatic fibrosis. *Toxicol Appl Pharmacol*. 2016;294:43-53.

37. Peng YY, He YH, Chen C, et al. NLRC5 regulates cell proliferation, migration and invasion in hepatocellular carcinoma by targeting the Wnt/beta-catenin signaling pathway. *Cancer Lett*. 2016;376(1):10-21.

SUPPORTING INFORMATION

Additional supporting information can be found online in the Supporting Information section at the end of this article.